UNIVERSITY OF LEEDS

This is a repository copy of *Technical note: Optimization functions for re-irradiation treatment planning*.

White Rose Research Online URL for this paper:
https://eprints.whiterose.ac.uk/208225/

Version: Accepted Version

Article:
Ödén, J., Eriksson, K., Svensson, S. et al. (6 more authors) (2024) Technical note: Optimization functions for re-irradiation treatment planning. Medical Physics, 51 (1). pp. 476-484. ISSN 0094-2405

https://doi.org/10.1002/mp.16815

Reuse
Items deposited in White Rose Research Online are protected by copyright, with all rights reserved unless indicated otherwise. They may be downloaded and/or printed for private study, or other acts as permitted by national copyright laws. The publisher or other rights holders may allow further reproduction and re-use of the full text version. This is indicated by the licence information on the White Rose Research Online record for the item.

Takedown
If you consider content in White Rose Research Online to be in breach of UK law, please notify us by emailing eprints@whiterose.ac.uk including the URL of the record and the reason for the withdrawal request.

White Rose university consortium
Universities of Leeds, Sheffield & York

eprints@whiterose.ac.uk
https://eprints.whiterose.ac.uk/

Technical note: Optimization functions for re-irradiation treatment planning

Jakob Ödén[1], Kjell Eriksson[1], Stina Svensson[1], John Lilley[2], Christopher Thompson[2], Christopher Pagett[2], Ane Appelt[2, 4], Louise Murray[3, 4], Rasmus Bokrantz[1]

[1]RaySeach Laboratories AB, Stockholm, Sweden
[2]Department of Medical Physics and Engineering, Leeds Cancer Centre, St. James' University Hospital, Leeds, United Kingdom
[3]Department of Clinical Oncology, Leeds Cancer Centre, St. James' University Hospital, Leeds, United Kingdom
[4]Leeds Institute of Medical Research at St James's, University of Leeds, Leeds, United Kingdom

Running title: Re-irradiation optimization functions

Corresponding author
Jakob Ödén, PhD
RaySearch Laboratories AB
Eugeniavägen 18C
113 68 Stockholm, Sweden
jakob.oden@raysearchlabs.com

ABSTRACT

Background: Although re-irradiation is increasingly used in clinical practice, almost no dedicated planning software exists.

Purpose: Standard dose-based optimization functions were adjusted for re-irradiation planning using accumulated equivalent dose in 2-Gy fractions (EQD2) with rigid or deformable dose mapping, tissue-specific α/β, treatment-specific recovery coefficients, and voxelwise adjusted EQD2 penalization levels based on the estimated previously delivered EQD2 ($EQD2_{deliv}$).

Methods: To demonstrate proof-of-concept, 35 Gy in 5 fractions was planned to a fictious spherical relapse planning target volume (PTV) in three separate locations following previous prostate treatment on a virtual human phantom. The PTV locations represented one repeated irradiation scenario and two re-irradiation scenarios. For each scenario, three re-planning strategies with identical PTV dose-functions but various organ at risk (OAR) EQD2-functions was used:

1) $reRT_{regular}$: Regular functions with fixed EQD2 penalization levels larger than $EQD2_{deliv}$ for all OAR voxels.
2) $reRT_{reduce}$: As $reRT_{regular}$, but with lower fixed EQD2 penalization levels aiming to reduce OAR EQD2.
3) $reRT_{voxelwise}$: As $reRT_{regular}$ and $reRT_{reduce}$, but with voxelwise adjusted EQD2 penalization levels based on $EQD2_{deliv}$.

PTV near-minimum and near-maximum dose ($D_{98\%}/D_{2\%}$), homogeneity index (HI), conformity index (CI) and accumulated OAR EQD2 (α/β=3 Gy) were evaluated.

Results: For the repeated irradiation scenario, all strategies resulted in similar dose distributions. For the re-irradiation scenarios, $reRT_{reduce}$ and $reRT_{voxelwise}$ reduced accumulated average and near-maximum EQD2 by ~1-10 Gy for all relevant OARs compared to $reRT_{regular}$. The reduced OAR doses for $reRT_{reduce}$ came at the cost of distorted dose distributions with $D_{98\%}$=92.3%, HI=12.0%, CI=73.7% and normal tissue hot spots ≥150% for the most complex scenario, while $reRT_{regular}$ ($D_{98\%}$=98.1%, HI=3.2%, CI=94.2%) and $reRT_{voxelwise}$ ($D_{98\%}$=96.9%, HI=6.1%, CI=93.7%) fulfilled PTV coverage without hot spots.

Conclusions: The proposed re-irradiation specific EQD2-based optimization functions introduces novel planning possibilities with flexible options to guide the trade-off between target coverage and OAR sparing with voxelwise adapted penalization levels based on $EQD2_{deliv}$.

Keywords: re-irradiation; optimization functions; equivalent dose

1. INTRODUCTION

Radiotherapy treatment to a previously irradiated volume, so-called re-irradiation, is a promising technique, used in an increasing number of patients in a large variety of treatment sites.[1] Although few definitive guidelines exist and high-quality re-irradiation prospective data are lacking,[1–3] several of the well-recognized challenges associated with re-irradiation have been studied. These include the need to retrieve accurate image and dose data, handling of anatomical changes between the radiotherapy courses, integration of radiobiology when summing multiple radiotherapy courses, and deciding on clinically relevant dose constraints.[3–7] In contrast, almost no planning software specifically designed for re-irradiation exists, and even fewer efforts have been made on creating re-irradiation-specific optimization functions. Instead, various approaches requiring multiple manual steps for dose extraction and dose summation are often used.[4,6] Slightly more complex planning methods also exist where radiobiologically meaningful approaches are employed using, for example, the biological effective dose or the equivalent dose in 2-Gy fractions (EQD2).[8] Recent studies within the Support Tool for Re-Irradiation Decisions guided by Radiobiology (STRIDeR) project have, however, addressed some of these re-irradiation specific planning issues including early versions of the optimization functions presented here, which act on the 3D distribution of the accumulated EQD2.[3,4] Beyond acting on radiobiologically meaningful doses, other key issues when using standard optimization functions in re-irradiation planning are the lack of accounting for tissue recovery between treatment courses, and the use of penalization dose levels without accounting for the estimated previously delivered EQD2 ($EQD2_{deliv}$). In particular, the latter is an issue in situations where the previously delivered dose in a voxel is similar or higher than the requested total EQD2 level, which might cause misbehavior in the optimization as very low, or even negative, voxel doses are requested.

In this study, optimization functions adapted to re-irradiation treatment planning are presented in detail. The adapted functions act on accumulated EQD2, use tissue- and treatment course specific recovery coefficients, and voxelwise adapted EQD2 penalization levels as a function of $EQD2_{deliv}$. Beyond this, the implementation includes feedback on the optimized EQD2 metrics during optimization, and the option to override the $EQD2_{deliv}$ in an organ with a user-defined EQD2 if dose accumulation uncertainty is considered too large (e.g., due to uncertainties in the deformable image registration (DIR)).

2. METHODS

The proposed optimization functions designed for re-irradiation treatments were implemented in a research version of the treatment planning system RayStation 11A (RaySearch Laboratories AB, Stockholm, Sweden) and are described in the paragraphs below.

2.1. Re-irradiation optimization functions

The re-irradiation optimization functions are based on the EQD2 using the linear-quadratic model for cell survival. The use of EQD2 allows for dose summation of radiotherapy courses with different fractionation schedules and is often used for dose summations in re-irradiation treatments.[1,3,4,9]

2.1.1. Equivalent dose

For a total dose (D) consisting of equal fractionation doses (d), the EQD2 is expressed as,

$$\mathrm{EQD2} = D \cdot \frac{\alpha/\beta + d}{\alpha/\beta + 2}, \tag{1}$$

where α/β is an endpoint- and radiation quality-specific parameter that describes the sensitivity to changes in the dose per fraction. For re-irradiation planning, the total accumulated EQD2 ($\mathrm{EQD2_{tot}}$) should be accounted for,

$$\mathrm{EQD2_{tot}} = \mathrm{EQD2_{reRT}} + \sum_{j=1}^{J} (1 - r_j) \cdot \mathrm{EQD2_{deliv,\,j}}, \tag{2}$$

where $\mathrm{EQD2_{reRT}}$ is the EQD2 from the planned re-irradiation treatment, J is the number of previous treatment courses, and r_j and $\mathrm{EQD2_{deliv,\,j}}$ is the recovery coefficient and $\mathrm{EQD2_{deliv}}$ for treatment course j, respectively. The organ- and treatment course specific recovery coefficient is a simplified way to account for partial time-dependent tissue recovery between the radiotherapy courses,[10,11] and lies between 0 and 1 (where zero reflects no recovery and one full recovery of the organ). The current implementation allows up to three unique user-defined recovery coefficients for each optimization function.

2.1.2. Dose accumulation

The implementation here supports both rigid and DIR for dose mapping.[3,4] Note that the previously delivered dose from course j in Eq. (2) can be estimated in various ways including the planned dose, dose-tracking on daily images, etc., and is always mapped to the re-irradiation CT before voxel-by-voxel conversion to $\mathrm{EQD2_{deliv,\,j}}$ with region of interest (ROI)-specific α/β ratios and ROI and treatment course specific recovery coefficients. Note also that the re-irradiation optimization function methodology presented in this study is conceptually invariant to the methodology used for dose accumulation. Hence, for simplicity and keeping focus on the optimization functions, the $\mathrm{EQD2_{deliv}}$ was estimated from the planned dose using the same CT for both the primary and the re-irradiation treatments for the studied virtual human phantom case. Challenges with image registration for dose mapping has previously been discussed in a general context[12] and specifically for re-irradiation.[3]

2.1.3. Re-irradiation optimization functions

The standard physical optimization functions that impose a one-sided quadratic penalty on voxel dose deviations from a desired dose level[13] were adjusted for re-irradiation treatment planning to penalize the $EQD2_{tot}$ (from Eq. (2)) deviations from a desired EQD2 level ($EQD2_{level}$). To accommodate optimization issues related to voxels where $EQD2_{deliv}$ is similar or higher than the desired $EQD2_{level}$, the $EQD2_{level}$ was further allowed to be adjusted per ROI in a voxelwise fashion to account for the $EQD2_{deliv}$ with a minimum allowed unpenalized EQD2 level for the re-irradiation treatment ($EQD2_{reRTmin}$) as,

$$EQD2^*_{level,\,i} = \max_{i \in ROI} \left\{ EQD2_{level,\,i},\ EQD2_{deliv,\,i} + EQD2_{reRTmin} \right\}, \tag{3}$$

where $EQD2^*_{level,\,i}$ is the adjusted EQD2 penalization level for voxel i and $EQD2_{deliv,\,i}$ is the estimated delivered EQD2 for voxel i. If the voxelwise adjustment is *not* selected, Eq. (3) is simply reduced to $EQD2^*_{level,\,i} = EQD2_{level,\,i}$, where $EQD2_{level,\,i}$ is the regular EQD2 penalization level for voxel i. A schematic 1D representation of the $EQD2^*_{level}$, with and without this voxelwise adjustment to the $EQD2_{deliv}$, is shown in

Figure 1 for a maximum EQD2 function and a EQD2-fall off function. In other aspects the re-irradiation functions behave as the standard dose-based optimization functions, which can be used in combination with the re-irradiation functions. The implementation was made for all standard optimization functions f in RayStation, which in their adapted form may be written as

$$f = \omega \cdot \sum_{i=1}^{N} g(EQD2_{tot,\,i},\ EQD2^*_{level,\,i}) \cdot v_i \cdot \left(\frac{EQD2_{tot,\,i} - EQD2^*_{level,\,i}}{EQD2^*_{level,\,i}} \right)^2, \tag{4}$$

where ω is the function weight, v_i is the relative volume of voxel i of an ROI consisting of N number of voxels, and $EQD2_{tot,\,i}$ and $EQD2^*_{level,\,i}$ are the total EQD2 and adjusted EQD2 penalization level for voxel i calculated with Eqs. (2) and (3), respectively. The function g is given by $g(EQD2_{tot,\,i}, EQD2^*_{level,\,i}) = H(EQD2_{tot,\,i} - EQD2^*_{level,\,i})$, where H is the Heaviside step function, for fall-off and maximum EQD2 functions, by $g(EQD2_{tot,\,i}, EQD2^*_{level,\,i}) = H(EQD2^*_{level,\,i} - EQD2_{tot,\,i})$ for minimum EQD2 functions and by $g(EQD2_{tot,\,i}, EQD2^*_{level,\,i}) = 1$ for uniform dose functions. The fall-off functions here use a linearly decreasing $EQD2_{level}$ outside of the target region until a selected distance from the target edge. From thereon, the $EQD2_{level}$ is constant and equal to the lowest selected $EQD2_{level}$ for the function. Note, although not used in this study, the corresponding optimization functions using equivalent uniform dose and dose-volume histograms (DVHs) were also adapted accordingly for re-irradiation.

An example of the adapted dialog for adding the functions including the re-irradiation specific parameters is shown in Supplementary Figure 1. To allow flexibility if e.g. the

uncertainty in the dose mapping is considered to be too large due to anatomy changes, the user can override the accumulated $EQD2_{deliv}$ in Eq. (2) with one out of two options; (1) the minimum $EQD2_{deliv}$ to the 0.1 cm^2 of the ROI volume receiving the highest doses, or (2) any user-specified EQD2 value. If one of these options is selected (using corresponding check box or text box in Supplementary Figure 1), Eq. (2) is automatically simplified to $EQD2_{tot} = EQD2_{reRT} + EQD2_{oride}$ where $EQD2_{oride}$ is the override value used for all voxels in the ROI.

2.2. Re-irradiation treatment planning

To demonstrate proof-of-concept of the novel re-irradiation functions, a fictious prostate photon dual volumetric modulated arc therapy (VMAT) treatment of 60 Gy in 20 fractions (EQD2 = 72 Gy with α/β = 3 Gy) was planned on a virtual human male pelvis CIRS 801-P phantom (CIRS, Inc., Norfolk, VA, USA). The clinical target volume (CTV) consisted of the prostate and seminal vesicles and the planning target volume (PTV) was created as an isotropic expansion of the CTVs (1 cm for seminal vesicles and 0.5 cm for prostate). Beyond this, the rectum, bladder, small bowel, and femoral heads were delineated and considered as organs at risk (OARs).

Subsequently, a fictious spherical relapse gross tumor volume (GTV) of about 38 cm^3 (radius of 2.1 cm) was positioned in three distinct locations with identical coordinates in the superior-inferior direction to schematically represent 'repeat irradiation' (RI), 're-irradiation type 2' (RIT2), and 're-irradiation type 1' (RIT1) scenarios as defined by a recent European consensus report on re-irradiation[1]. The volume of the GTV corresponds to the median pelvic re-irradiation GTV from a systematic review on hypofractionated pelvic re-irradiation,[14] and the selected locations were inspired by the patterns of pelvic relapses[15] but had no anatomical meaning. In line with the recent increased interest in hypofractionated and ablative re-irradiation treatments,[14,16,17] three dual-arc VMAT plans of 35 Gy in 5 fractions (EQD2 = 70 Gy with α/β = 3 Gy) were optimized for each relapse PTV (3 mm isotropic expansion of the corresponding GTV) using the full 3D dose distribution from the first treatment course as the estimated previously delivered dose (i.e. $EQD2_{deliv}$ in Eq. (2)). As for the first treatment course, a voxel size of 2x2x2 mm^3 was used. The three re-planning strategies used an identical uniform PTV dose objective of 35 Gy but differed in the use of the novel re-irradiation functions for the OARs:

(1) $reRT_{regular}$: A regular EQD2 fall-off function acting on the whole phantom outline was combined with regular EQD2-based maximum objective functions for the bladder, rectum, small bowel, and the femoral heads *without* using the voxelwise adapted $EQD2^*_{level}$ in Eq. (3). Instead, a fixed $EQD2^*_{level} = EQD2_{deliv,max} + EQD2_{reRTmin}$ Gy was used in Eq. (4) for the maximum functions, where $EQD2_{deliv,\,max}$ is the maximum estimated delivered EQD2 to the OAR of interest and $EQD2_{reRTmin} \in [1, 10]$ Gy was selected depending on the relapse PTV

location and OAR. Hence, all voxels for each maximum OAR function had a fixed $EQD2^*_{level} > EQD2_{deliv}$.

(2) $reRT_{reduce}$: As (1) but with a fixed $EQD2^*_{level}$ per maximum OAR function of $EQD2^*_{level} = EQD2_{deliv,\,25\%}$ used in Eq. (4), where $EQD2_{deliv,\,25\%}$ denotes the minimum $EQD2_{deliv}$ to the 25% of the OAR receiving the highest $EQD2_{deliv}$, aiming to further reduce $EQD2_{tot}$ compared to (1). Hence, ¾ of the voxels for each maximum OAR function had $EQD2^*_{level} > EQD2_{deliv}$ and ¼ had $EQD2^*_{level} \leq EQD2_{deliv}$.

(3) $reRT_{voxelwise}$: Combining OAR objectives from (1) and (2) with $EQD2_{level}$ equal to the $EQD2^*_{level}$ from (2) per OAR with the corresponding OAR $EQD2_{reRTmin}$ from (1) as input to the voxelwise adaptation of $EQD2^*_{level}$ in Eq. (3). Hence, all voxels for each OAR had a voxelwise adjusted $EQD2^*_{level} > EQD2_{deliv}$ for the fall-off function and the maximum OAR functions.

Supplementary Figure 2 shows the optimization functions used for all three re-planning strategies in the RIT1 scenario including visualization of the optimized $EQD2_{tot}$ metrics to guide the user during re-irradiation optimization.

2.3. Plan evaluation

The PTV coverage of the re-irradiation plans was evaluated using $D_{98\%}$, $D_{2\%}$, the homogeneity index $\left(HI = \frac{D_{2\%} - D_{98\%}}{D_{50\%}}\right)$ and the conformity index $\left(CI = \frac{2 \cdot |TV \cap V_{target}|}{|TV| + |V_{target}|}\right)$, where $D_{x\%}$ is the minimum dose to $x\%$ of the PTV receiving the highest doses, the sets TV and V_{target} denote the treated volume and target volume, respectively, and $|A|$ is the volume of a set A. The TV was defined as the volume of the 98% isodose line. The clinical PTV goals were $D_{98\%} \geq 95\%$ of 35 Gy and $D_{2\%} \leq 105\%$ of 35 Gy, HI ≤ 10%, and CI ≥ 90%.

Subsequently, all re-irradiation plans were converted to $EQD2_{reRT}$ and summed with the $EQD2_{deliv}$ of the first treatment course using Eq. (2) with $r = 0$ and $\alpha/\beta = 3$ Gy for all voxels giving $EQD2_{tot}$. DVHs using $EQD2_{tot}$ were evaluated for the rectum, bladder, small bowel, and the femoral heads including comparisons of the average $EQD2_{tot}$ and the near-maximum $EQD2_{tot}$ ($EQD2_{tot,\,2\%}$).

3. RESULTS

Figure 1 shows schematical 1D examples of the implementation of the EQD2-based re-irradiation optimization functions for the maximum and fall-off functions used in $reRT_{regular}$, $reRT_{reduce}$ and $reRT_{voxelwise}$. Note that the $EQD2^*_{level}$ is lower than the $EQD2_{deliv}$ for large parts in Figure 1a for $reRT_{reduce}$ and in

Figure 1b, for both $reRT_{regular}$ and $reRT_{reduce}$, since the $EQD2^*_{level}$ is not using the novel voxelwise adjustment in Eq. (3). For $reRT_{voxelwise}$, the $EQD2^*_{level}$ instead adapts voxelwise to $EQD2_{deliv}$ with an offset equal to $EQD2_{reRTmin}$ (equal to 4 Gy in Figure 1) for voxels where $EQD2_{level} < EQD2_{deliv} + EQD2_{reRTmin}$ according to Eq. (3).

Figure 2 shows the EQD2 distribution for the first treatment course together with the superimposed EQD2 distributions for the three scenarios for each treatment strategy. Figure 3 shows the corresponding DVHs for the PTVs (using RI, RIT1 and RIT2 doses only) and two relevant OARs (using $EQD2_{tot}$) for each relapse scenario. The evaluated PTV dose metrices are summarized in Table 1. For the RI scenario, all three plans had similar EQD2 distributions and OAR doses (Figure 2 and Figure 3b) and fulfilled the clinical goals with similar dose metrics (Table 1 and Figure 3a). For the more complex re-irradiation scenarios RIT1 and RIT2, note the generally reduced EQD2 to the OARs for $reRT_{reduce}$ and $reRT_{voxelwise}$ compared to $reRT_{regular}$ (Figure 2). As indicated by Figure 3c and Figure 3d the largest reductions were achieved with $reRT_{reduce}$ where the average $EQD2_{tot}$ and $EQD2_{tot,\ 2\%}$ for the OARs were generally reduced by about 1-10 Gy and 3-12 Gy, respectively, compared to $reRT_{regular}$. For $reRT_{voxelwise}$, the corresponding OAR reductions compared to $reRT_{regular}$ were about 1-4 Gy in the average $EQD2_{tot}$ and 2-8 Gy in the $EQD2_{tot,\ 2\%}$. For $reRT_{voxelwise}$, this OAR sparing was achieved with comparable PTV coverage to $reRT_{regular}$ (Table 1 and Figure 3a) without adding any extra optimization time, while for $reRT_{reduce}$, the OAR sparing distorted the dose distributions causing PTV underdosage and increased HI for RIT1, and lowered the CI with normal tissue hot spots from the re-irradiation treatment alone of over 100 Gy EQD2 for both RIT1 and RIT2 (Table 1, Figure 2c, and Figure 3a).

4. DISCUSSION

The proposed optimization functions introduce a novel and flexible approach to re-irradiation treatment planning that account for accumulated estimated previously delivered dose in a radiobiologically meaningful way by using summed EQD2 across multiple treatment courses with tissue-specific recovery coefficients and α/β ratios. During the recent ESTRO Physics workshop on re-irradiation,[7] such dose accumulation capability (together with visualization) was identified as one of the highest priorities when scoring potential software tools to support safe clinical re-irradiation. Although some previous studies have reported similar approaches for the evaluation of re-irradiation treatments,[18,19] few have incorporated such functionalities into re-irradiation planning using commercially available software.[3,4]

For the fictitious RI scenario in this study, the three re-planning strategies performed equally well (Table 1, Figure 2, Figure 3a and Figure 3b), which was expected due to the large distances between PTV and relevant OARs associated with RI treatments.[1] However, note the

slightly elongated EQD2 distribution for $reRT_{reduce}$ compared to $reRT_{regular}$ and $reRT_{voxelwise}$ for the RI scenario. This is due to the large penalty associated with the OAR voxels where $EQD2^{*}_{level} < EQD2_{deliv}$ (¼ of the voxels for each OAR in this case), where the optimization formulation corresponds to a request for negative voxel doses since the desired EQD2 is lower than the already estimated delivered EQD2. Although this issue has minor impact in the RI scenario, it is the main reason for the markedly elongated dose distributions with normal tissue hot spots reaching over 100 Gy EQD2 for $reRT_{reduce}$ in the RIT1 and RIT2 scenarios (Figure 2c), which also caused the suboptimal PTV coverage in RIT1 (Table 1 and Figure 3a). This is also reflected in the evaluated OAR function values shown in Supplementary Figure 2 for the RIT1 scenario, where all maximum OAR function values are substantially higher for $reRT_{reduce}$ compared to $reRT_{regular}$ and $reRT_{voxelwise}$. That said, the accumulated OAR EQD2 is lowest for $reRT_{reduce}$, as shown by the feedback of the minimum $EQD2_{tot}$ at 0.1 cm^3 in Supplementary Figure 2 and by the DVHs in Figure 3d. The high function values, extremely elongated dose distributions, normal tissue hot spots, and target underdosage are strong arguments to avoid regular re-irradiation optimization functions with $EQD2^{*}_{level} < EQD2_{deliv}$. While the selection of $EQD2_{level} = EQD2_{deliv,\ 25\%}$ for $reRT_{reduce}$ was somewhat arbitrary, comparable outcomes could have been achieved as long as $EQD2_{level}$ remained below $EQD2_{deliv}$ for certain voxels. However, if the selected ratio of voxels with $EQD2^{*}_{level} < EQD2_{deliv}$ were gradually reduced from ¼, the PTV coverage would be improved with a more symmetric dose distribution, fewer hot spots, and lower OAR function values. However, finding the optimal trade-off might be a time-consuming effort, and should be avoided as negative doses are requested as long as $EQD2^{*}_{level} < EQD2_{deliv}$ in some voxels. This is both unphysical and undesirable from an optimization point of view since the re-irradiation dose contribution cause large penalties due to the quadratic formulation of the objective functions (see Eq. (4) and Supplementary Figure 2).

Instead, the $reRT_{regular}$ planning strategy ensured $EQD2^{*}_{level} > EQD2_{deliv}$ for all voxels for the maximum OAR functions. However, the OAR sparing of $reRT_{regular}$ was substantially worse compared to the $reRT_{reduce}$ strategy (Figure 3). To handle this, the favorable attributes of the two other re-planning strategies were combined by introducing the voxelwise adapted $EQD2^{*}_{level}$ for $reRT_{voxelwise}$. This resulted in satisfactory PTV coverage (Table 1) while simultaneously avoiding the suboptimal solutions of $reRT_{regular}$ (insufficiently strict on OAR doses) and $reRT_{reduce}$ (excessively strict on OAR doses causing normal tissue hot spots) for the complex re-irradiation scenarios (Figure 2 and Figure 3). By using the override-option where the $EQD2_{deliv}$ in an ROI is replaced with a suitable fixed EQD2, one can in some cases produce similar plans as the $reRT_{voxelwise}$ strategy by setting a fixed $EQD2^{*}_{level} = EQD2_{reRTmin} + EQD2_{oride}$. However, since the spatial information of the $EQD2_{deliv}$ is then lost, this option should only be used in cases where the 3D dose mapping is not used due to e.g. large DIR uncertainties.

This study focused on the optimization function design and some specific options using a phantom case without consideration of DIR for dose mapping, recovery coefficients, tissue-specific α/β values, multiple treatment courses etc. For such simplified scenarios, it might often be possible to generate acceptable re-irradiation treatment plans using regular dose-based functions, although this was beyond the scope in this study. However, this is often more time-consuming, involves multiple manual steps and becomes extremely challenging in clinical reality when dealing with anatomical changes between treatment courses, heterogeneously delivered doses from several treatment courses of varying fractionation schedules, with different recovery coefficients and tissue-specific α/β.[4,6] Hence, it can be argued that the functions presented here are of greatest benefit when the re-irradiation complexity increases since manual procedures then becomes extremely troublesome and time-consuming. This is indicated by recent studies using preliminary EQD2-based optimization functions in a full clinical re-irradiation workflow within the STRIDeR project.[3,4] Moreover, since the α/β and recovery coefficients are selected for each optimization function (see Supplementary Figure 1 and Supplementary Figure 2), an ongoing study is exploring optimization strategies that mitigates against uncertainties in these parameters. Beyond this, the implementation also allows exploration of optimization strategies that are robust against uncertainties in delivered dose by e.g. use of an estimated worst case delivered dose in the optimization to account for uncertainties in the dose delivery, DIR, and dose mapping.

5. CONCLUSIONS

The proposed optimization functions introduce novel and flexible approaches for re-irradiation treatment planning which can combine EQD2- and dose-based functions without adding time in the optimization stage. The key features of the re-irradiation functions are:

- Voxelwise dose accumulation of multiple treatment courses to estimate accumulated EQD2, which is used in re-irradiation optimization based on rigid or DIR for dose mapping, with tissue specific α/β ratios, and tissue- and treatment course specific recovery coefficients.
- An ROI-specific and voxel-specific EQD2 penalization level adjusted for the estimated previously delivered EQD2, specifying the additionally allowed EQD2 for the re-irradiation treatment.
- The option to use a uniform ROI-specific previously delivered EQD2 if the dose mapping is considered unreliable.
- Feedback on the optimized EQD2 metrics during optimization.

CONFLICT OF INTEREST

The current work is an output from a formal research collaboration between Leeds Teaching Hospitals NHS Trust and RaySearch Laboratories AB. Kjell Eriksson is also a shareholder in RaySearch Laboratories AB.

ACKNOWLEDGEMENT

Ane Appelt and Louise Murray are currently Associate Professors funded by Yorkshire Cancer Research (award numbers L389AA and L389LM). Authors from Leeds would also like to acknowledge Cancer Research UK funding for the Leeds Radiotherapy Research Centre of Excellence (RadNet; C19942/A28832).

REFERENCES

1. Andratschke N, Willmann J, Appelt AL, et al. European Society for Radiotherapy and Oncology and European Organisation for Research and Treatment of Cancer consensus on re-irradiation: definition, reporting, and clinical decision making. *Lancet Oncol*. 2022;23(10):e469-e478. doi:10.1016/S1470-2045(22)00447-8
2. Nieder C, Andratschke NH, Grosu AL. Increasing frequency of reirradiation studies in radiation oncology: systematic review of highly cited articles. *Am J Cancer Res*. 2013;3(2):152-158. https://www.ncbi.nlm.nih.gov/pmc/articles/PMC3623835/.
3. Nix M, Gregory S, Aldred M, et al. Dose summation and image registration strategies for radiobiologically and anatomically corrected dose accumulation in pelvic re-irradiation. *Acta Oncol*. 2022;61(1):64-72. doi:10.1080/0284186X.2021.1982145
4. Murray L, Thompson C, Pagett C, et al. Treatment plan optimisation for reirradiation. *Radiother Oncol*. 2023;182:109545. doi:10.1016/j.radonc.2023.109545
5. Lee DS, Woo JY, Kim JW, Seong J. Re-irradiation of hepatocellular carcinoma: Clinical applicability of deformable image registration. *Yonsei Med J*. 2016;57(1):41-49. doi:10.3349/ymj.2016.57.1.41
6. Paradis KC, Matuszak MM. The Medical Physics Management of Reirradiation Patients. *Semin Radiat Oncol*. 2020;30(3):204-211. doi:10.1016/j.semradonc.2020.02.008
7. Vasquez Osorio E, Mayo C, Jackson A, Appelt A. Challenges of re-irradiation: A call to arms for physicists - and radiotherapy vendors. *Radiother Oncol*. 2023;182:109585. doi:10.1016/j.radonc.2023.109585
8. McVicar N, Thomas S, Liu M, Carolan H, Bergman A. Re-irradiation volumetric modulated arc

therapy optimization based on cumulative biologically effective dose objectives. *J Appl Clin Med Phys*. 2018;19(6):341-345. doi:10.1002/acm2.12481

9. Bentzen SM, Dörr W, Gahbauer R, et al. Bioeffect modeling and equieffective dose concepts in radiation oncology-Terminology, quantities and units. *Radiother Oncol*. 2012;105(2):266-268. doi:10.1016/j.radonc.2012.10.006

10. Armstrong S, Hoskin P. Complex Clinical Decision-Making Process of Re-Irradiation. *Clin Oncol*. 2020;32(11):688-703. doi:10.1016/j.clon.2020.07.023

11. Das S, Patro KC, Mukherji A. Recovery and Tolerance of the Organs at Risk during Re - irradiation. 2023:23-28. doi:10.4103/jco.jco

12. Murr M, Brock KK, Fusella M, et al. Applicability and usage of dose mapping/accumulation in radiotherapy. *Radiother Oncol*. 2023;182:109527. doi:10.1016/j.radonc.2023.109527

13. Oelfke U, Bortfeld T. Inverse planning for photon and proton beams. *Med Dosim*. 2001;26(2):113-124. doi:10.1016/S0958-3947(01)00057-7

14. Murray LJ, Lilley J, Hawkins MA, Henry AM, Dickinson P, Sebag-Montefiore D. Pelvic re-irradiation using stereotactic ablative radiotherapy (SABR): A systematic review. *Radiother Oncol*. 2017;125(2):213-222. doi:10.1016/j.radonc.2017.09.030

15. Brand DH, Parker JI, Dearnaley DP, et al. Patterns of recurrence after prostate bed radiotherapy. *Radiother Oncol*. 2019;141:174-180. doi:10.1016/j.radonc.2019.09.007

16. Mantel F, Flentje M, Guckenberger M. Stereotactic body radiation therapy in the re-irradiation situation - a review. *Radiat Oncol*. 2013;8(1):1-13. doi:10.1186/1748-717X-8-7

17. Munoz F, Fiorica F, Caravatta L, et al. Outcomes and toxicities of re-irradiation for prostate cancer: A systematic review on behalf of the Re-Irradiation Working Group of the Italian Association of Radiotherapy and Clinical Oncology (AIRO). *Cancer Treat Rev*. 2021;95(November 2020):102176. doi:10.1016/j.ctrv.2021.102176

18. Brooks ED, Wang X, De B, et al. An algorithm for thoracic re-irradiation using biologically effective dose: a common language on how to treat in a "no-treat zone." *Radiat Oncol*. 2022;17(1):1-11. doi:10.1186/s13014-021-01977-1

19. Meijneke TR, Petit SF, Wentzler D, Hoogeman M, Nuyttens JJ. Reirradiation and stereotactic radiotherapy for tumors in the lung: Dose summation and toxicity. *Radiother Oncol*. 2013;107(3):423-427. doi:10.1016/j.radonc.2013.03.015

FIGURES AND TABLES

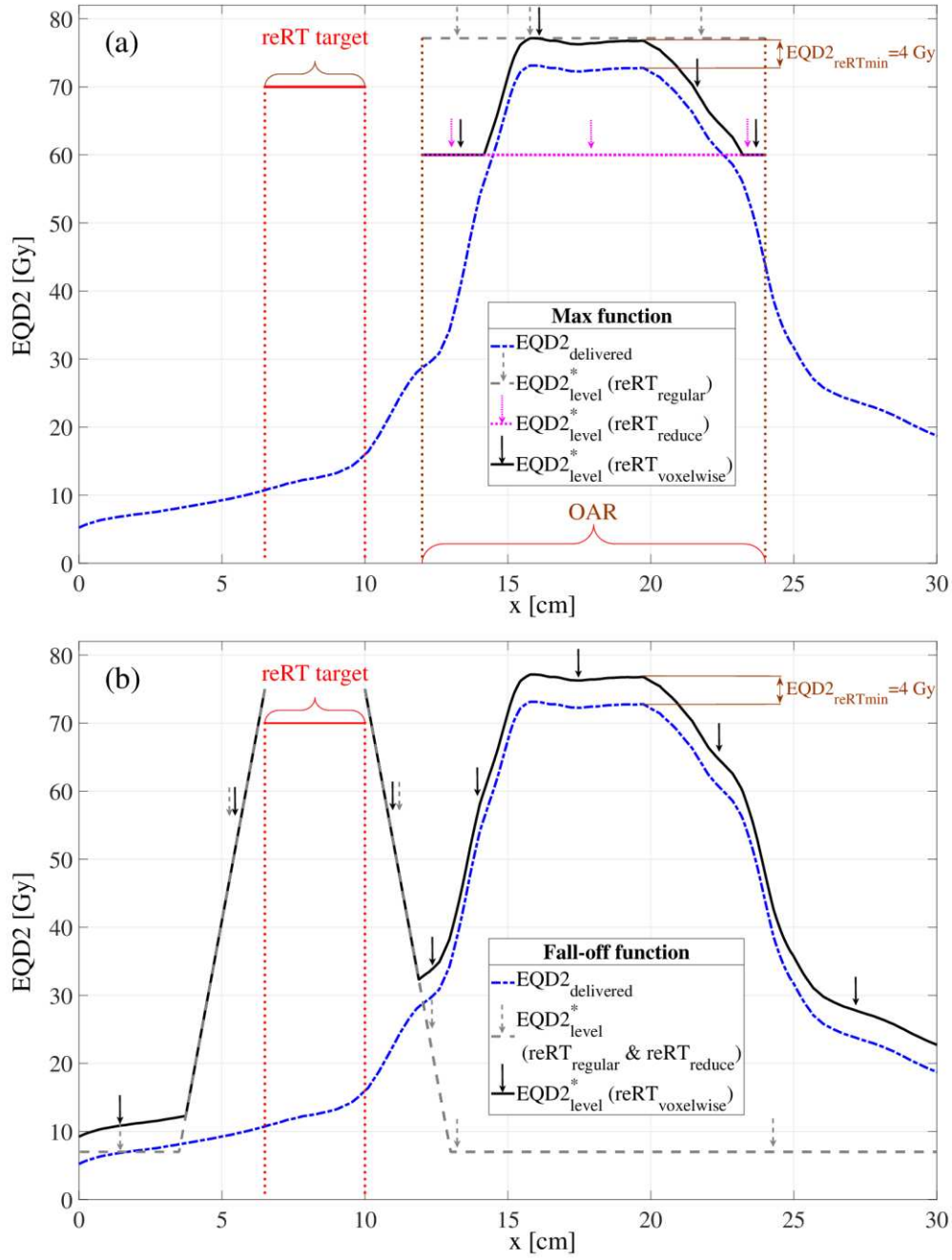

Figure 1. Schematic 1D illustrations of the adjusted equivalent dose in 2-Gy fraction (EQD2) penalization levels ($EQD2^*_{level}$) with an additionally allowed unpenalized re-irradiation (reRT) EQD2 ($EQD2_{reRTmin}$) of 4 Gy used in the planning of $reRT_{regular}$, $reRT_{reduce}$ and $reRT_{voxelwise}$. (a): a maximum EQD2 function with $EQD2_{level}$ of 60 Gy for an organ at risk (OAR) and (b): a EQD2 fall-off function linearly decreasing from 75 Gy at the reRT target edge to 7 Gy at 3 cm distance (constant beyond). The reRT target is marked in red with an estimated previously delivered EQD2 ($EQD2_{deliv}$) as dashed-dotted blue lines, the $EQD2^*_{level}$ for $reRT_{regular}$ and $reRT_{reduce}$ as dashed grey or dotted magenta lines with corresponding arrows, and the novel implementation of the voxelwise adjusted $EQD2^*_{level}$ for $reRT_{voxelwise}$ as solid black lines with black arrows. The arrows show that the optimization will aim to reduce the total EQD2 below the $EQD2^*_{level}$ for each re-planning strategy. An α/β of 3 Gy was assumed to calculate EQD2 for all voxels.

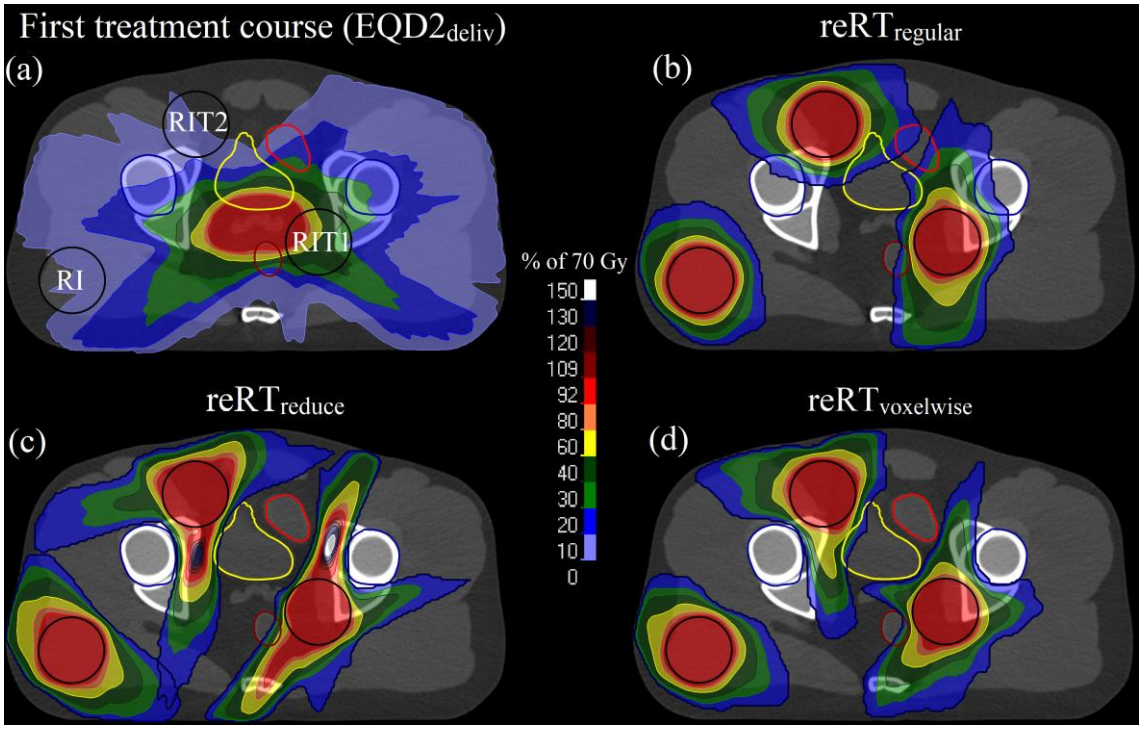

Figure 2. (a): The equivalent dose in 2-Gy fraction (EQD2) distribution of the first treatment course ($EQD2_{deliv}$) with the three fictious relapse planning target volumes (PTVs) marked in black; RI (repeat irradiation), RIT1 (re-irradiation type 1) and RIT2 (re-irradiation type 2). The superimposed EQD2 distributions for the three relapse scenarios are shown for (b) $reRT_{regular}$, (c) $reRT_{reduce}$ and (d) $reRT_{voxelwise}$. The EQD2 was truncated at 14 Gy (20% iso-EQD2 line) to avoid overlap, leaving only a minor overlap of the 20% iso-EQD2 line of RI and RIT2 in (c). The contours of bladder, rectum, small bowel, and femoral heads are marked in yellow, brown, red, and blue, respectively. The EQD2 distributions were calculated using an $\alpha/\beta = 3$ Gy for all voxels. 92% and 109% of 70 Gy EQD2 approximately corresponds to 95% and 105% of 35 Gy in 5 fractions, respectively.

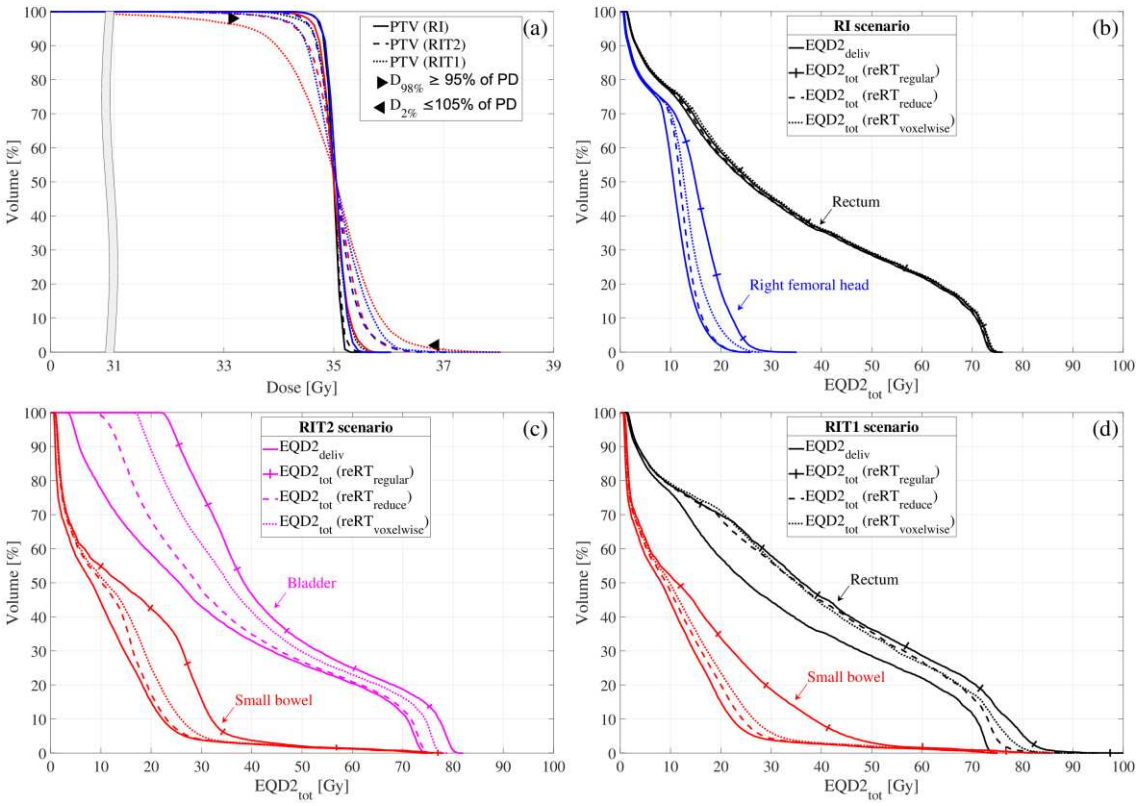

Figure 3. Dose-volume histograms (DVHs) using dose and total equivalent dose in 2-Gy fraction ($EQD2_{tot}$) for the three relapse scenarios – repeat irradiation (RI), re-irradiation type 1 (RIT1) and type 2 (RIT2). (a): DVHs for the planning target volumes (PTV) with a broken x-axis for $reRT_{regular}$ (black lines), $reRT_{reduce}$ (red lines) and $reRT_{voxelwise}$ (blue lines) for all three relapse scenarios with the PTV coverage goals marked as horizontal black triangles. [(b), (c), and (d)]: DVHs of two organs at risk per relapse scenario for the first treatment course ($EQD2_{deliv}$) in full lines and the $EQD2_{tot}$ for $reRT_{regular}$ (full lines with perpendicular crossing lines), $reRT_{reduce}$ (dashed lines) and $reRT_{voxelwise}$ (dotted lines). (b): The RI scenario, (c): the RIT2 scenario and (d): the RIT1 scenario. The EQD2 was calculated using an α/β = 3 Gy for all voxels.

Table 1. Dose evaluation metrices for the planning target volume (PTV) for all relapse scenarios and re-planning strategies.

Relapse scenario	Re-planning strategy	$D_{98\%}$ [%]	$D_{2\%}$ [%]	HI [%]	CI [%]
Repeat irradiation (RI)	$reRT_{regular}$	99.1	100.5	1.4	92.4
	$reRT_{reduce}$	98.5	101.4	2.8	93.3
	$reRT_{voxelwise}$	99.0	100.9	1.9	93.0
Re-irradiation type 2 (RIT2)	$reRT_{regular}$	99.1	100.8	1.7	92.8
	$reRT_{reduce}$	96.8	102.6	5.8	84.1
	$reRT_{voxelwise}$	98.3	102.7	4.4	93.4
Re-irradiation type 1 (RIT1)	$reRT_{regular}$	98.1	101.3	3.2	94.2
	$reRT_{reduce}$	92.3	104.3	12.0	73.7
	$reRT_{voxelwise}$	96.9	103.0	6.1	93.7

$D_{x\%}$ = minimum dose to x% of the PTV receiving the highest doses; CI = conformity index; HI = homogeneity index

460

SUPPLEMENTARY MATERIAL

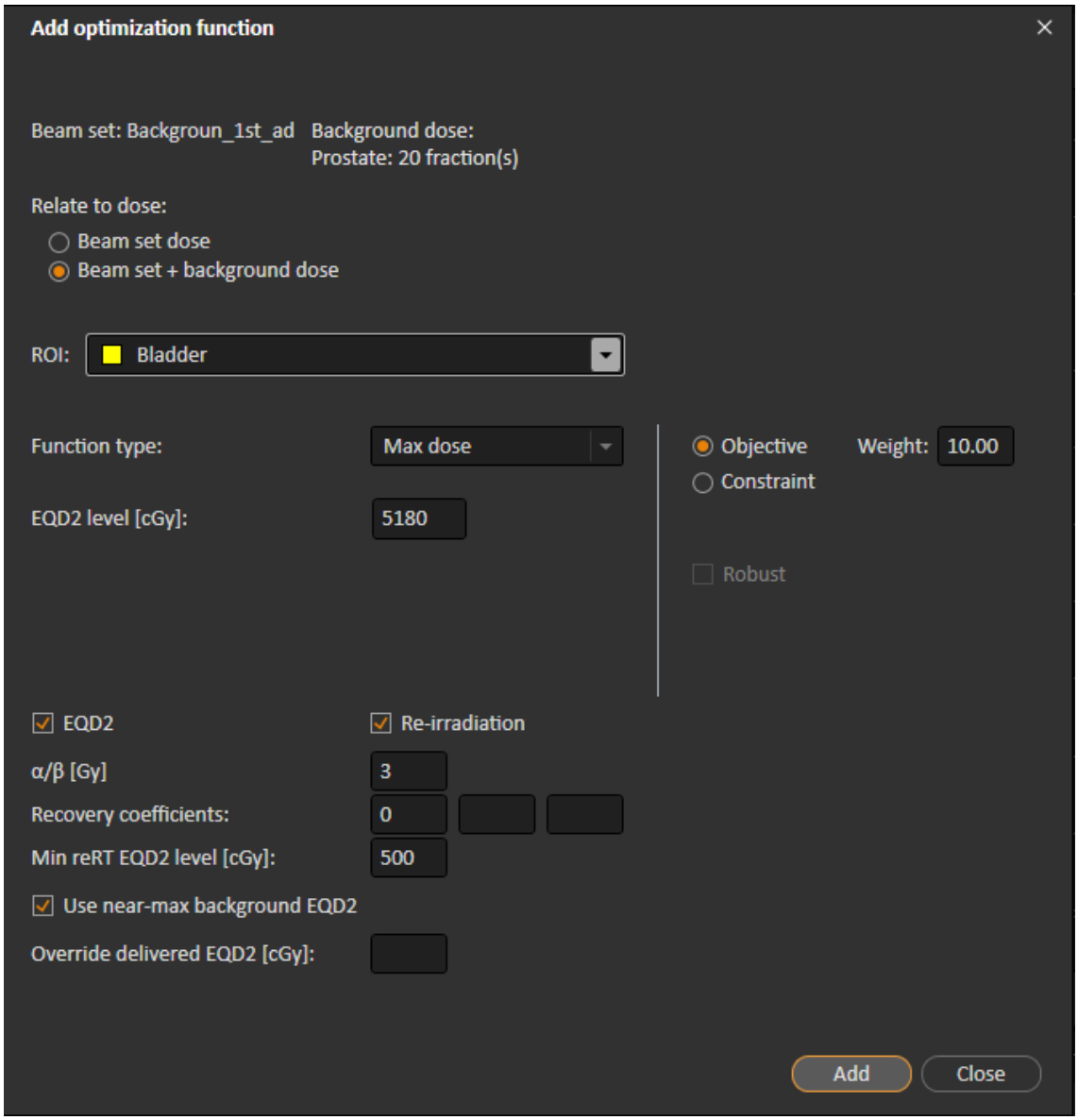

Supplementary Figure 1. The adapted dialog in the research version of RayStation v11A for adding an optimization function. The user selects region of interest (ROI) for the function, function type, function weight, objective or constraint function, and if the function should use the beam set dose only or the accumulated dose including the estimated delivered dose. The user then selects the re-irradiation specific settings; the penalization level in equivalent dose in 2-Gy fractions ($EQD2_{level}$), α/β ratio, recovery coefficients, the minimum allowed unpenalized re-irradiation EQD2 ($EQD2_{reRTmin}$), and whether to override the estimated previously delivered EQD2 ($EQD2_{deliv}$) in Eq. (2) with a fixed EQD2 using one out of two options; (1) the minimum $EQD2_{deliv}$ to the 0.1 cm^2 of the ROI volume receiving the highest doses, or (2) any user-specified EQD2 value.

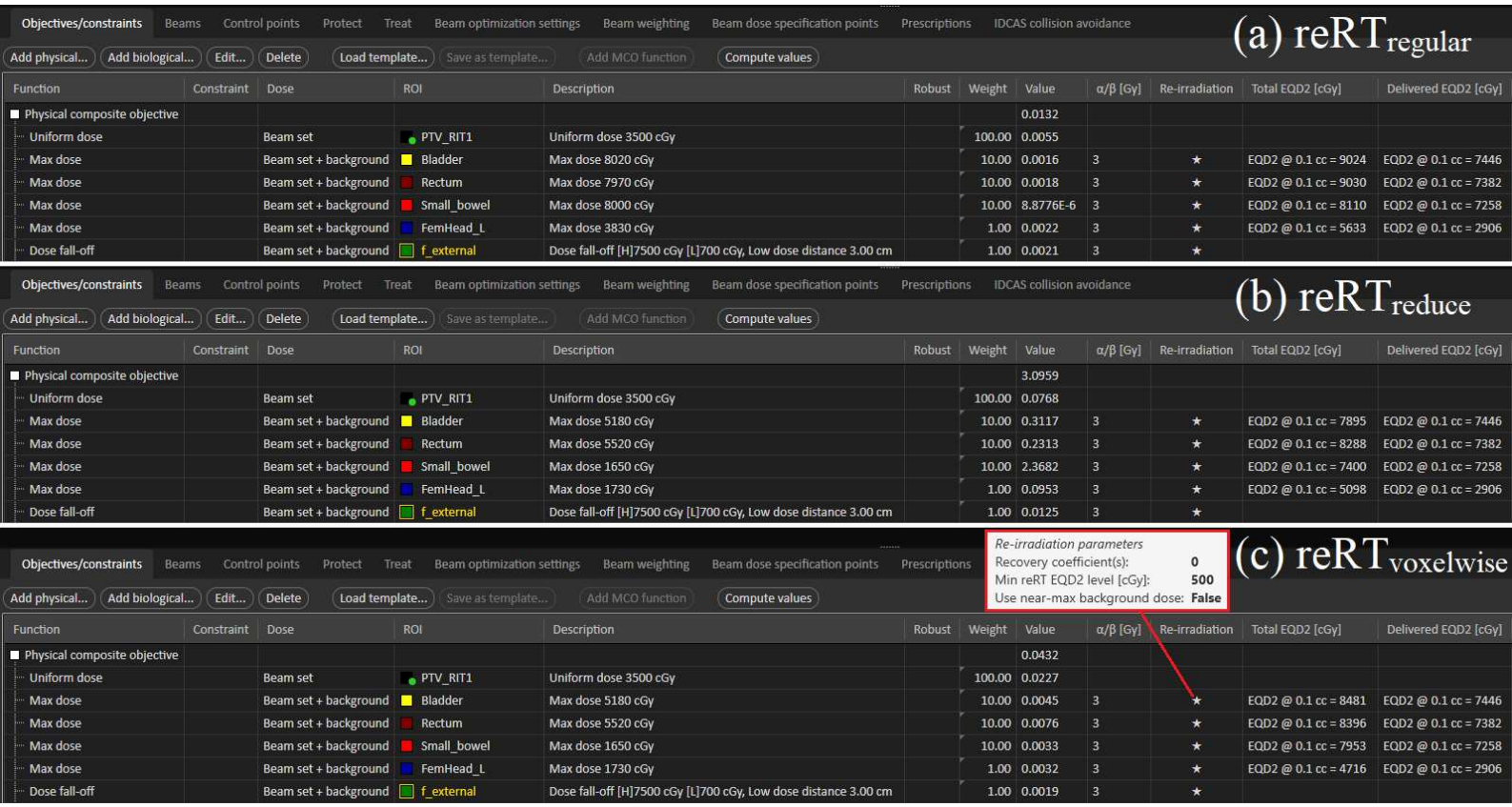

Supplementary Figure 2. Example of the optimization function lists in the research version of RayStation v11A for (a) $reRT_{regular}$, (b) $reRT_{reduce}$ and (c) $reRT_{voxelwise}$ used for optimization of the type 1 re-irradiation (RIT1) scenario. The uniform target objective is dose-based, while all organs at risk (OARs) objectives use the novel re-irradiation functions acting on the total equivalent dose in 2-Gy fractions ($EQD2_{tot}$). The function value (calculated using the final dose distribution) and selected function parameters from Supplementary Figure 1 are seen for each function in the list including the re-irradiation specific parameters. The α/β ratio is shown in a separate column, while a mouse-over the corresponding ★ triggers a tooltip with the added re-irradiation function parameters as seen in (c) for the bladder maximum function. The final two columns on the right supply feedback during optimization of the corresponding EQD2 metric for the total EQD2 and the estimated previously delivered EQD2. For the maximum functions, the feedback metric is the minimum $EQD2_{deliv}$ to the 0.1 cm^2 of the ROI volume receiving the highest doses, as seen in (a), (b) and (c) while no such feedback is given for the EQD2 fall-off function.